Assessing the impact of climate change on dissolved oxygen using a flow field ecosystem model that takes into account the anaerobic and aerobic environment of bottom sediments

Koue, Jinichi

(Citation)
Acta Geochimica,44(1):11-22

(Issue Date)
2025-02

(Resource Type)
journal article

(Version)
Version of Record

Acta Geochim
https://doi.org/10.1007/s11631-024-00711-4

ORIGINAL ARTICLE

Assessing the impact of climate change on dissolved oxygen using a flow field ecosystem model that takes into account the anaerobic and aerobic environment of bottom sediments

Jinichi Koue[1]

Received: 13 April 2024 / Revised: 12 May 2024 / Accepted: 4 June 2024

Abstract This study examines the potential impacts of climate change on Lake Biwa, Japan's largest freshwater lake, with a focus on temperature, wind speed, and precipitation variations. Leveraging data from the IPCC Sixth Assessment Report, including CCP scenarios, projecting a significant temperature rise of 3.3–5.7 °C in the case of very high GHG emission power, the research investigates how these shifts may influence dissolved oxygen levels in Lake Biwa. Through a one-dimensional model incorporating sediment redox reactions, various scenarios where air temperature and wind speed are changed are simulated. It is revealed that a 5 °C increase in air temperature leads to decreasing 1–2 mg/L of dissolved oxygen concentrations from the surface layer to the bottom layer, while a decrease in air temperature tends to elevate 1–3 mg/L of oxygen levels. Moreover, doubling wind speed enhances surface layer oxygen but diminishes it in deeper layers due to increased mixing. Seasonal variations in wind effects are noted, with significant surface layer oxygen increases from 0.4 to 0.8 mg/L during summer to autumn, increases from 0.4 to 0.8 mg/L in autumn to winter due to intensified vertical mixing. This phenomenon impacts the lake's oxygen cycle year-round. In contrast, precipitation changes show limited impact on oxygen levels, suggesting minor influence compared to other meteorological factors. The study suggests the necessity of comprehensive three-dimensional models that account for lake-specific and geographical factors for accurate predictions of future water conditions. A holistic approach integrating nutrient levels, water temperature, and river inflow is deemed essential for sustainable management of Lake Biwa's water resources, particularly in addressing precipitation variations.

Keywords Climate change · Dissolved oxygen · Sediment redox reaction · Stratification · Water quality

1 Introduction

The progression of global warming has been reported by the IPCC, and there is a need to promote adaptation measures based on this progression (IPCC 2022). Regarding the assessment of climate change impact on the oceans, ocean-scale studies have been mainly conducted on sea surface temperature rise (Fueglistaler and Silvers 2021), sea level rise (Jevrejeva et al. 2016; Tebaldi et al. 2021), and ocean acidification (Byrne and Hernández 2020; Findlay and Turley 2021). On the other hand, in coastal areas and lakes, where spatio-temporal changes are inherently large, it is difficult to extract clear impacts due to historical instrument biases as well as by sparse observing system coverage (Cheng et al. 2016; Durack et al. 2018), although some inner bays and lakes have been confirmed to have trends in sea water temperature and lake water temperature increase (Johnson and Lyman 2020). In recent years, however, there have been discussions on the effects on physical structures such as stratification and mass transport in coastal areas and lakes (Robins et al. 2014; Ross et al. 2015; Yang et al. 2015), on water quality such as eutrophication (Rabalais et al. 2009; Statham 2012), and on ecosystems (Scavia et al. 2002). For example, the frequency of occurrence of anoxic water masses is increasing in closed water bodies from rising temperatures due to climate change (Smucker et al.

✉ Jinichi Koue
koue@maritime.kobe-u.ac.jp

[1] Graduate School of Maritime Sciences, Kobe University, 5-1-1 Fukaeminami, Higashinada-ku, Kobe, Hyogo 658-0022, Japan

Published online: 26 June 2024

2021). In addition, the change to a subtropical climate is causing changes in the stratification structure of the oceans and lakes due to low-pressure systems with large, strong winds (Stetler et al. 2021). In addition, the pattern of river entry into estuaries changes depending on changes in river discharge associated with precipitation, and the addition of land use changes in river basins changes the pattern of entry (Yang et al. 2015; Christianson et al. 2020), increases in river discharge (Rabalais et al. 2009), and other findings have been obtained.

Hypoxia, the phenomenon of reduced dissolved oxygen (DO), is a water quality problem that adversely affects marine and lake ecosystems, and the decrease in DO is more pronounced in coastal areas, which receive pollution load from rivers, than in the open ocean, and it is not easy to elucidate the causes of anoxia. Many studies on anoxia and oxygen cycling have been conducted in closed water bodies that are subject to anthropogenic pollution, such as Lake Biwa, which is the target area of this study (Detmer et al. 2022; Desgué-Itier et al. 2023; Perlov et al. 2023). In recent study, it is conducted a water quality future projection for the ocean and showed that phytoplankton occurring in the surface layer of the ocean in the world will decrease (Henson et al. 2021). Such changes are expected to have a significant impact on the oxygen cycle structure and the dissipation of anoxic water masses in Lake Biwa, which is known to have high oxygen consumption due to the decomposition of organic matter. However, there have been few studies that have quantitatively evaluated the impact of global warming on Lake Biwa's anoxia or focused on the spatial distribution of anoxic water masses. Therefore, the first objective of this study is to quantitatively clarify the DO circulation structure in the bottom layer of Lake Biwa by conducting a one-dimensional flow-water quality simulation for the lake. The second objective is to examine the effects of climatic changes (temperature, wind speed, and precipitation) on the future disappearance of anoxic water masses in Lake Biwa and changes in the DO circulation structure.

2 Methodology

2.1 Simulation model

2.1.1 Computational domain

Figure 1 illustrates the simulation domain employed in this model. At the monitoring point of Imazu-oki (35°23′41″ N, 136°07′57″ E), located in the northern region of Lake Biwa, the largest freshwater lake in Japan, an observation station was established to assess water temperature stratification and the bottom sediment environment in a meticulous manner. A vertical unequal mesh was deployed, extending from the lake's surface to a depth of approximately 90 m. To achieve a detailed evaluation, the grid configuration varied according to depth.

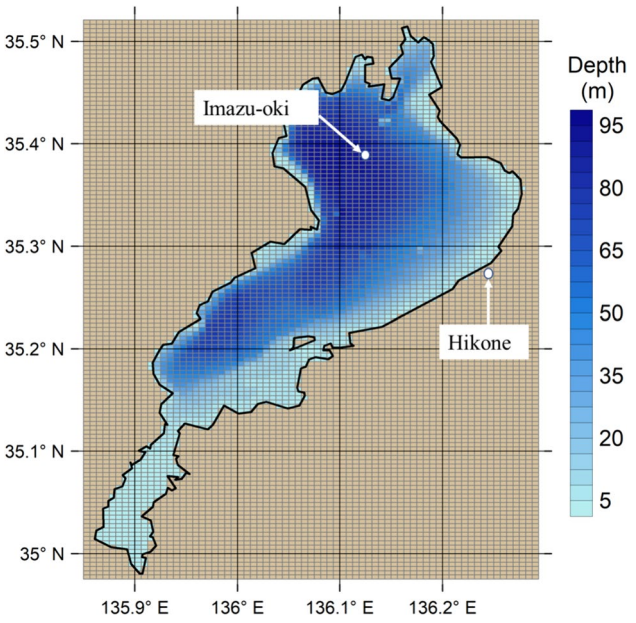

Fig. 1 Calculation domain in Lake Biwa: the monitoring point of observation: Imazu-oki, the meteorological observationpoint: Hikone

From the lake's surface down to a depth of 20 m, the grid size was fixed at 0.5 m. Subsequently, the grid size underwent a gradual increase from 20 to 55 m, reaching a maximum of 2.5 m, with increments of 0.1 m. In the depth range of 55–87 m, the grid size was systematically reduced from 2.5 m to a minimum of 0.1 m at 0.1 m intervals. Finally, from a depth exceeding 87 m down to the lake bed at 90 m, the grid size was maintained at 0.1 m. It is noteworthy that the vertical axis (z-axis) was oriented upwards in this configuration.

2.1.2 Calculation period

The designated calculation period spanned from April 1, 2006, to March 31, 2014. The initial year was specifically allocated as a warm-up phase, while the subsequent 7 years, spanning from April 1, 2007, to March 31, 2014, were delineated as the formal evaluation period. The temporal resolution for the calculations was established at a granularity of 1 s.

2.2 Hydrodynamics model

In the present study, a novel vertical one-dimensional model was formulated, drawing upon the foundation laid by the three-dimensional hydrodynamic model proposed by Koue et al. (2018) and the ecosystem model developed by Koue

et al. (2020). The hydrodynamic component of the model computes flow direction, flow velocity, and water temperature at each mesh point. The newly introduced ecosystem model incorporates 11 state variables, encompassing "phytoplankton (Chlorophyll-a, b, and c)," "zooplankton," "suspended organic matter," "dissolved organic matter," "ammonium nitrogen (NH_4-N)," "nitrite nitrogen (NO_2-N)," "nitrate nitrogen (NO_3-N)," "phosphate phosphorus (PO_4-P)," "dissolved oxygen (DO)," "total nitrogen (T-N)," and "total phosphorus (T-P)," and quantifies changes in their concentrations. Furthermore, to simulate oxygen consumption in sediment, an additional sediment model was incorporated as a sub-model in this investigation.

The specific details of the construction of the one-dimensional hydrodynamic model are outlined herein.

2.2.1 Basic equations

The flow field model employed in this study comprised a vertical one-dimensional diffusion equation, a hydrostatic pressure approximation equation, and a diffusion equation governing water temperature. The fundamental equations are presented herewith. The one-dimensional diffusion equation for vertical flow is expressed as follows:

$$\frac{\partial u}{\partial t} = \nu_z \frac{\partial^2 u}{\partial z^2} \tag{1}$$

$$\frac{\partial v}{\partial t} = \nu_z \frac{\partial^2 v}{\partial z^2} \tag{2}$$

The hydrostatic pressure approximation is formulated as follows,

$$0 = -\frac{1}{\rho_0}\frac{\partial p}{\partial z} - \frac{\rho}{\rho_0} g \tag{3}$$

The heat diffusion equation is expressed as follows,

$$\frac{\partial T}{\partial t} = \kappa_z \frac{\partial^2 T}{\partial z^2} \tag{4}$$

The calculation of density is elucidated as follows,

$$\rho = 1000.07 - 0.00469(T - 273.15)^2 - 0.0035(T - 273.15) \tag{5}$$

The determination of vertical eddy viscosity and eddy diffusion coefficient is conducted as follows,

$$Ri = -\frac{g}{\rho_0} \bullet \frac{\frac{\partial \rho}{\partial z}}{\left(\frac{\partial W}{\partial z}\right)^2} \tag{6}$$

$$\nu_z = \frac{0.0001}{1.0 + 5.2Ri} \tag{7}$$

$$\kappa_z = \frac{0.0001}{\left(1.0 + \frac{10}{3} \times Ri\right)^{\frac{3}{2}}} \tag{8}$$

In the context of the variables provided, where u and v denote horizontal velocities (m/s), W represents the magnitude of horizontal flow velocity (m/s), T denotes water temperature (K), p signifies pressure (N/m^2), ρ indicates the density of lake water (kg/m^3), ρ_0=10^3 is the density of reference lake water (kg/m^3), g stands for gravitational acceleration (m/s^2), ν_z represents vertical eddy viscosity (m^2/s), and κ_z represents vertical eddy diffusivity (m^2/s).

During the summer season, a thermocline is observed to form in Lake Biwa at a depth ranging from 10 to 20 m. Consequently, the values of ν_z and κ_z are derived utilizing the Richardson number (Ri), a dimensionless parameter that characterizes the flow's instability in the presence of layered density variations.

2.2.2 Meteorological data

Meteorological data for the analysis of heat balance on the lake surface and wind-induced surface shear stress were sourced from the Japan Meteorological Agency's observation and forecast data, commonly known as GPV data (Grid Point Value). The data encompassed parameters such as "temperature (K)," "pressure (Pa)," "wind direction and speed (m/s)," and "relative humidity (%)." Solar radiation observations were obtained from the Hikone Regional Meteorological Observatory, provided at hourly intervals (Fig. 1). The GPV data featured a grid spacing of 5 km. In this study, meteorological data from Imazu-oki were utilized, employing a weighted average inversely proportional to the square of the distance to obtain interpolated values. This meteorological dataset was updated on an hourly basis and employed in the hydrodynamic model calculations. The hourly updates contribute to a more intricate representation of heat balance and flow dynamics on the lake surface. Figure 2 a–c shows the average daily meteorological data observed at Hikone Meteorological Observatory from 2007 to 2014.

2.2.3 Initial conditions

The initial condition was established with a flow velocity set at 0 m/s. The initial water temperature on April 1, 2006, was determined through linear interpolation using data collected twice a month, specifically on March 20, 2006, and April 10, 2006. This data was systematically obtained by the Lake Biwa Environmental Research Institute at Imazu-oki, spanning depths of 0.5, 5, 10, 15, 20,

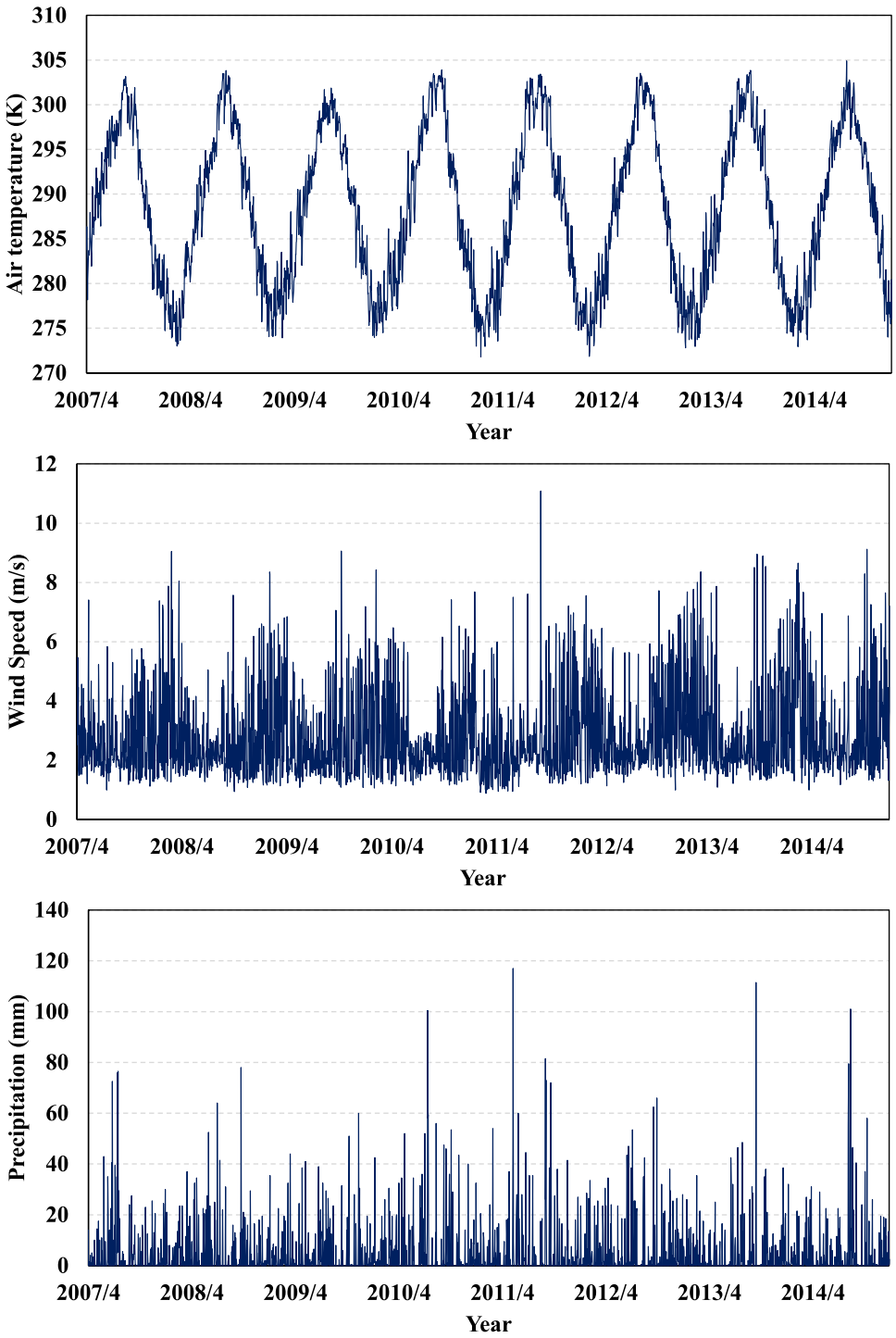

Fig. 2 The meteorological data observed at Hikone Meteorological Observatory from 2007 to 2014. **a** Daily mean of air temperature (℃), **b** daily mean of wind speed (m/s), **c** total daily precipitation (mm)

30, 40, 60, 80 m, and approximately 90 m across ten distinct locations. The values for April 1, 2006, were derived through linear interpolation based on the aforementioned data points from March 20, 2006, and April 10, 2006.

2.3 Water quality ecosystem model

The one-dimensional model employed for long-term analysis was constructed based on the three-dimensional water

quality model of Lake Biwa as developed by Koue et al. (2020). To facilitate a comprehensive examination of inorganic nutrient dynamics and dissolved oxygen consumption, inorganic nitrogen was segregated into state variables representing "ammonia-form nitrogen," "nitrite-form nitrogen," and "nitrate-form nitrogen." Similarly, inorganic phosphorus was compartmentalized into "phosphate-form phosphorus." The one-dimensional diffusion equation was utilized to solve the flow field, and leveraging the outcomes of the flow field model, a novel model was devised. This new model incorporated a bottom sediment model that accounts for anaerobic and aerobic processes in bottom mud sediments, amalgamated with a suspended ecosystem model that considers three types of phytoplankton.

In line with the flow calculations, a vertical one-dimensional model is employed for water quality calculations to ascertain the average concentration within each layer. Each constituent undergoes alterations resulting from chemical and biological processes, as well as diffusion. The temporal evolution is encapsulated by the following one-dimensional diffusion equation:

$$\frac{\partial C_i}{\partial t} = \kappa_z \frac{\partial^2 C_i}{\partial z^2} + Q_{C_i} \tag{9}$$

The left side denotes the time-varying term, while the right side encompasses the diffusion term and variations resulting from chemical and biological processes (Q_{C_i}). The state variables comprise the 11 components delineated in Table 1. A summary of the chemical and biological processes associated with each state variable is presented in Table 2. A bottom sediment model was constructed to model the behavior of nitrogen, phosphorus, and organic matter in bottom sediments. The state variables used in the bottom sediment model are listed in Table 3. The chemical and biological processes of each state variable are summarized in Table 4.

Table 1 Variables representing system states in ecosystem model

Element	Symbol	Unit
Phytoplankton	C_{PX}	μgC/L
Zooplankton	C_Z	μgC/L
Suspended organic matter	C_{POC}	mg/m^3
Dissolved organic matter	C_{DOC}	mg/m^3
Ammonia nitrogen	$C_{\mathrm{NH_4}N}$	mg/m^3
Nitrite nitrogen	C_{NO_2N}	mg/m^3
Nitrate nitrogen	C_{NO_3N}	mg/m^3
Phosphate-form phosphorus	C_{PO_4P}	mg/m^3
Dissolved oxygen	C_{DO}	mg/L
Total nitrogen	C_{TN}	mg/m^3
Total phosphorus	C_{TP}	mg/m^3
Total carbon	C_{TC}	mg/m^3

Table 2 Mass equilibrium of individual state variables within the ecosystem model

C_{PX}	Growth by photosynthesis − Extracellular secretion − Predation by zooplankton − Phytoplankton respiration − Dying − Sedimentation
C_Z	Growth by phytoplankton feeding − Zooplankton feces − Zooplankton excretion by respiration − Zooplankton death
C_{POC}	Phytoplankton die-off + zooplankton feces + natural mortality of zooplankton − mineralization of suspended-form organic matter − generation of decomposition surplus + sedimentation of suspended-form organic matter
C_{DOC}	Extracellular secretion + decomposition surplus generation − mineralization of dissolved organic matter by aerobic bacteria
$C_{\mathrm{NH_4N}}$	− Phytoplankton ingestion by photosynthesis + phytoplankton respiration + zooplankton excretion by respiration + mineralization of suspended organic matter + mineralization of dissolved organic matter by aerobic bacteria + leaching of nitrogen from bottom sediment − nitrification of ammonia-form nitrogen
$C_{\mathrm{NO_2N}}$	Nitrification of ammonia nitrogen − Nitrite nitrogen
$C_{\mathrm{NO_3N}}$	− Phytoplankton uptake by photosynthesis + nitrification and denitrification of nitrite nitrogen
$C_{\mathrm{PO_4P}}$	− Phytoplankton uptake by photosynthesis + phytoplankton respiration + zooplankton excretion by respiration + mineralization of suspended organic matter + mineralization of dissolved organic matter by aerobic bacteria + leaching of phosphorus from bottom sediment
C_{DO}	Supply by photosynthesis − Consumption by phytoplankton respiration − Consumption by zooplankton respiration − Oxygen consumption by suspended organic matter − Oxygen consumption by dissolved organic matter − Consumption in bottom mud + aeration − Oxygen consumption associated with nitrification of ammonia-form nitrogen − Oxygen consumption associated with nitrite-form nitrogen
C_{TN}	N/C ratio in phytoplankton × time variation of phytoplankton + N/C ratio in zooplankton × time variation of zooplankton + N/C ratio in suspended organic matter × time variation of suspended organic matter + N/C ratio in dissolved organic matter × time variation of dissolved organic matter + time variation of ammonia-form nitrogen + time variation of nitrite-form nitrogen + nitrate-form nitrogen
C_{TP}	P/C ratio in phytoplankton × time variation of phytoplankton + P/C ratio in zooplankton × time variation of zooplankton + P/C ratio in suspended organic matter × time variation of suspended organic matter + P/C ratio in dissolved organic matter × time variation of dissolved organic matter + time variation of phosphate form phosphorus
C_{TC}	Time variation of phytoplankton + time variation of zooplankton + time variation of suspended organic matter + time variation of dissolved organic matter

Table 3 Sediment model state variables

Element		Symbol	Unit
Sediment	Inorganic nitrogen	C_{MIN}	mg/m^3 dry mud
	Inorganic phosphorus	C_{MIP}	mg/m^3 dry mud
	Organic nitrogen	C_{MON}	mg/m^3 dry mud
	Organic phosphorus	C_{MOP}	mg/m^3 dry mud
	Organic matter	C_{MOC}	mg/m^3 dry mud
Pore water	Ammonia nitrogen	C_{WNH_4N}	mg/m^3
	Nitrite nitrogen	C_{WNO_2N}	mg/m^3
	Nitrate-nitrogen	C_{WNO_3N}	mg/m^3
	Inorganic phosphorus	C_{WIP}	mg/m^3
	Dissolved organic matter	C_{WOC}	mg/m^3
	Dissolved oxygen	C_{WDO}	mg/Ll

2.3.1 Initial conditions

The data utilized in the ecosystem model, including water temperature, flow direction, and flow velocity, were updated at 3-hour intervals using the computation results derived from the flow field model. Initial conditions for nutrients, such as nitrogen and phosphorus, were established based on bi-monthly observations conducted at Imazu-oki by the Lake Biwa Environmental Research Institute.

2.4 Scenario case for meteorological change

The Sixth Assessment Report (AR6) of the Intergovernmental Panel on Climate Change (IPCC) recommended several scenarios using a Shared Socio-economic Pathway (SSP) that complements the Representative Concentration Pathway (RCP) presented in the Fifth Assessment Report (AR5). The SSP makes detailed assumptions about greenhouse gas emissions potential as well as population and GDP etc., in addition to GHG emission capacities, with detailed assumptions on socio-economic development trends. Among these scenarios, the scenario with the highest GHG emission intensity (SSP 5-8.5) showed a high likelihood of a 3.3–5.7 ℃ increase in global average temperature at the end of the twenty-first century (2081–2100) (IPCC 2022), which is why the climate change scenarios in this study are conditional on a ± 5 °C change. The study assumes a ± 5 °C change in the climate change scenarios. In addition, the high projected likelihood of an increase in the frequency of very strong tropical cyclones (equivalent to 'fierce' typhoons) over the southern seas of Japan is conditioned on a doubling or halving of wind speeds on average. Working Group 2 (WG2) also addressed the impact of changes in precipitation on the hydrological cycle system (IPCC 2022). Therefore, in this study, conditions were also set for a doubling or halving of precipitation. By comparing the results of dissolved oxygen concentration in Lake Biwa under these condition settings, the predicted range of dissolved oxygen concentration in Lake Biwa in the future under each scenario can be estimated. Each scenario was defined as shown in Table 5 below.

3 Results and discussion

Figure 3a, b shows seasonal and inter-annual change of vertical distribution of observed and simulated water temperature at Imazu-oki from 2007 to 2014. Regarding seasonal changes in the vertical distribution of water temperature, the observed results and calculated values generally agreed. As for the inter-annual change in water temperature, although there was a slight difference between the observed and calculated values for water temperature in the thermocline, the observed and calculated values for the surface and bottom

Table 4 Concentration balance for each state variable in the sediment model

C_{MIN}	Sedimentation + decomposition of organic nitrogen in bottom mud (aerobic/anaerobic) + adsorption/desorption onto mud particles
C_{MIP}	Sedimentation + decomposition of organic phosphorus in bottom mud + adsorption/desorption on mud particles – adsorption/desorption on pore water (aerobic/anaerobic)
C_{MON}	Sedimentation – Decomposition of organic nitrogen in bottom mud (aerobic/anaerobic)
C_{MOP}	Sedimentation – Decomposition of organic phosphorus in bottom mud
C_{MOC}	Sedimentation – Dissolution of organic matter in bottom sediment
C_{WNH_4N}	Decomposition of organic nitrogen in bottom mud – Adsorption/desorption on mud particles + Diffusion – Nitrification of ammonia nitrogen
C_{WNO_2N}	Diffusion + Nitrification of ammonia nitrogen – Nitrification of nitrite nitrogen
C_{WNO_3N}	Diffusion + Nitrification of nitrite nitrogen – Denitrification of nitrate nitrogen
C_{WIP}	Decomposition of organic phosphorus in bottom mud – Adsorption/desorption on mud particles + diffusion + desorption from bottom mud (aerobic/anaerobic)
C_{WOC}	Dissolution of organic matter in sludge + diffusion – Decomposition of organic matter in pore water
C_{WDO}	Diffusion – Oxygen consumption by nitrification of ammonia nitrogen – Oxygen consumption by nitrite nitrogen – Oxygen consumption by decomposition of organic matter in pore water

Table 5 Scenarios in numerical experiments

Case name	Air temperature	Wind speed (m/s)	Wind direction (m/s)	Volume of precipitation
BASE	original	original	original	original
AT_+5 ℃	+5 ℃	Original	Original	Original
AT_−5 ℃	−5 ℃	Original	Original	Original
WS_double	Original	Double	original	original
WS_half	original	Half	original	original
Pre_double	original	original	original	Double
Pre_half	original	original	original	Half

layers generally agreed. In 2008, 2010, and 2013, it was observed that air temperatures tended to be higher than usual in the summer, and that water temperature stratification became stronger. Although it was a cool summer in 2009, a similar trend was observed when comparing calculated values and observed values. Figure 4 shows a comparison of seasonal change of vertical distribution of observed and simulated DO, at Imazu-oki in 2007. Figure 5 shows a comparison of inter-annual change of vertical distribution of observed and simulated DO, in the surface layer (0 m depth), thermocline (20 m depth) and deep layer (90 m depth) at Imazu-oki from 2007 to 2014.

In order to verify the accuracy of this ecosystem model, the numerical calculation results were compared with the measured data on the present amount of nutrients and DO that seem to have the greatest impact on the water quality environment in the inland lake. The numerical results generally represent seasonal increases and decreases, and seem to be in agreement with the quantitative results.

As the ambient air temperature increased, stratification became evident (Fig. 3a, b), leading to a decline in dissolved oxygen concentration. Initially sourced from the atmosphere and diffusing from the surface to the lower layer, dissolved oxygen experienced a reduction with the establishment of a thermocline characterized by a significant water temperature gradient. Consequently, the lower layer ceased to receive oxygen from external sources and relied solely on the decomposition of organic matter by bacteria, resulting in oxygen consumption (Fig. 4a).

In the upper layer, oxygen replenishment occurred through photosynthesis facilitated by plant cells within the region of light penetration, with atmospheric oxygen supply being the primary contributing factor. Consequently, the likelihood of oxygen depletion in the upper layer was lower compared to the bottom layer. Coinciding with the formation of a robust water temperature stratification, the depletion of oxygen persisted until approximately September. Subsequently, from autumn through winter, the breakdown of water temperature stratification, induced by declining temperatures, prompted oxygen supply from the surface layer. As a result, oxygen concentration rebounded during the full-layer circulation period in winter, approaching levels observed in the surface layer.

Figure 4b illustrates the interannual variation in dissolved oxygen concentration from April 2007 to March 2014. It is evident that saturated dissolved oxygen concentration correlated with water temperature, as surface water temperature varied in tandem with annual air temperature fluctuations. Additionally, wind-induced stirring in the surface layer impacted dissolved oxygen concentration fluctuations within the thermocline and surface layer.

In the lower layer, instances of elevated temperatures beyond the norm, attributed to annual temperature variations, intensified water temperature stratification, impeding oxygen supply from the surface layer. This phenomenon was particularly notable in the years 2008, 2010, and 2013, resulting in a diminished oxygen concentration in the bottom layer. Furthermore, heightened sedimentation of organic matter in certain years contributed to increased oxygen consumption. A comparison of observed and calculated values reveals a general consistency with these trends.

Figure 5 shows the interannual variation in the difference in dissolved oxygen concentrations between the temperature-change case and the baseline case from 2007 to 2014. When temperature was increased by 5 °C, dissolved oxygen concentrations in the surface layer decreased by about 0.8–1.2 mg/L, near the thermocline by 0.9–1.5 mg/L and near the bottom layer by 0.6–1.2 mg/L. Oxygen concentrations were least likely to decrease in the bottom layer, with dissolved oxygen concentrations decreasing more near the thermocline than in the surface layer. The reason why the oxygen concentration was least likely to decrease in the bottom layer may be that the bottom layer is less affected by atmospheric temperature than the surface layer. Near the surface layer, the water is in contact with the atmosphere, so it is also affected by air temperature, but there is a direct oxygen supply from the atmosphere. Near the thermocline, the water temperature fluctuates widely and the rate of decrease in saturated dissolved oxygen concentration at 15–20 °C is high, which may have resulted in more hypoxia. When the temperature decreased by 5 °C, the dissolved oxygen concentration in the surface layer increased by about 0.8–1.5 mg/L, and by the same amount in the vicinity of the thermocline. In the bottom layer, the dissolved oxygen concentration increases by about 0.8–2.5 mg/L. It is characteristic that the rate of increase in oxygen concentration in the bottom layer is decreasing year by year, but this is because the saturated dissolved oxygen concentration itself is also increasing because the water temperature in the bottom layer is decreasing every year.

Figure 6 shows the interannual variation of the dissolved oxygen concentration difference between the case

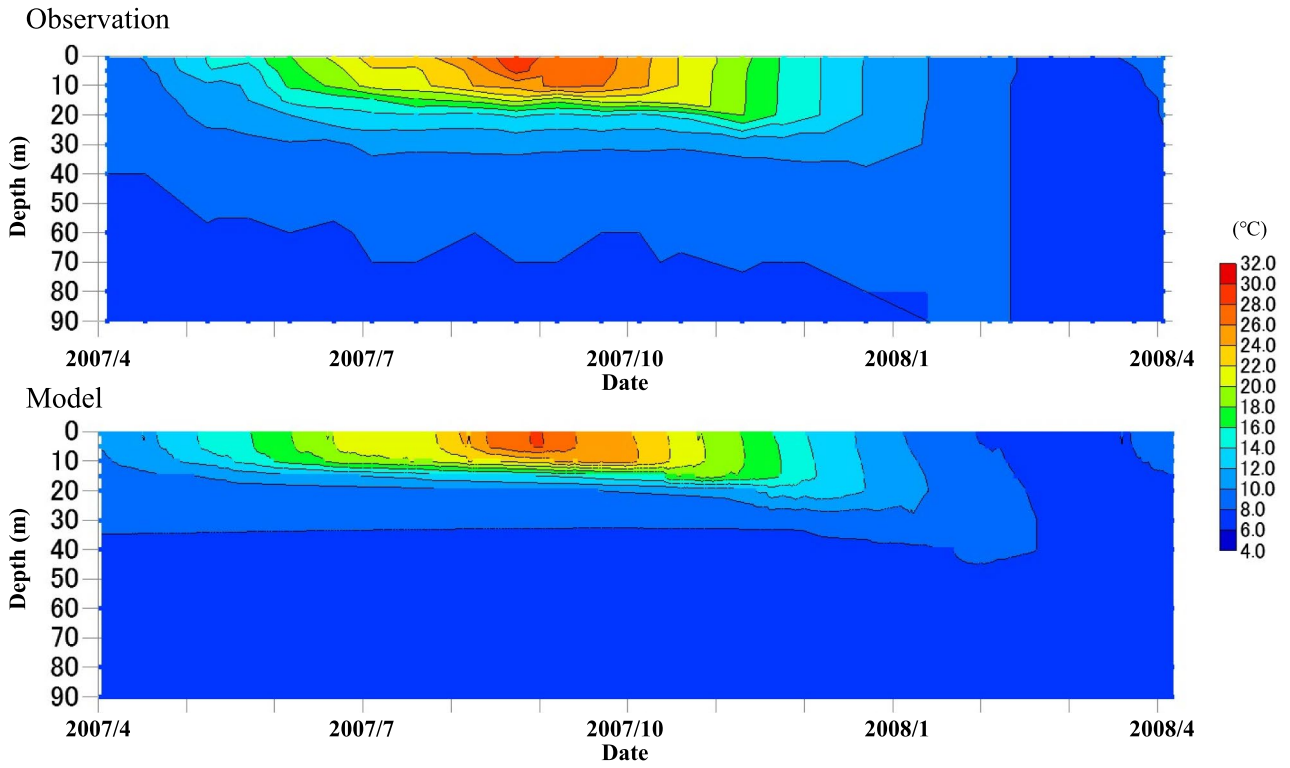

(a) Seasonal change of vertical distribution of water temperature in 2007

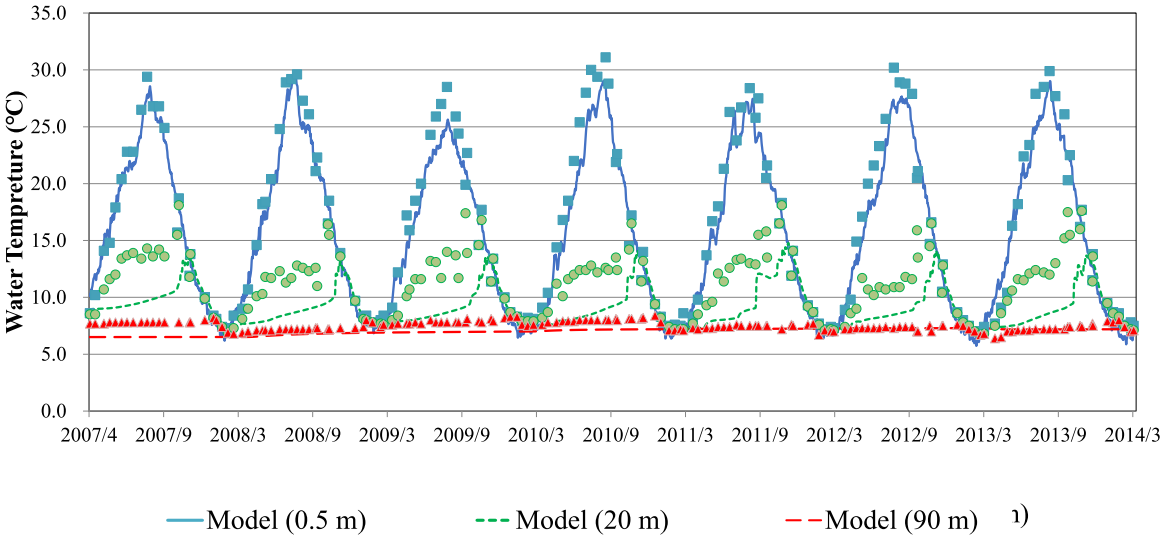

(b) Inter-annual change of vertical distribution of water temperature

Fig. 3 Seasonal and inter-annual change of vertical distribution of observed and simulated water temperature at Imazu-oki

with varying wind speed and the baseline case from 2007 to 2014. When wind speed was increased by a factor of two, dissolved oxygen concentrations increased by about 0.2–0.4 mg/L in the surface layer, with a higher rate of increase during the summer and autumn months. Dissolved oxygen concentrations in the water temperature in the thermocline varied in the range − 0.5–0.4 mg/L. The decrease in dissolved oxygen concentration during the summer season was due to increased wind velocity, which stirred up the surface layer and mixes it with the thermocline, resulting in higher water temperatures, lower saturated dissolved oxygen concentrations and a decrease in oxygen concentrations. Oxygen concentrations in the bottom layer fluctuated in the range of − 0.6–0.4 mg/L,

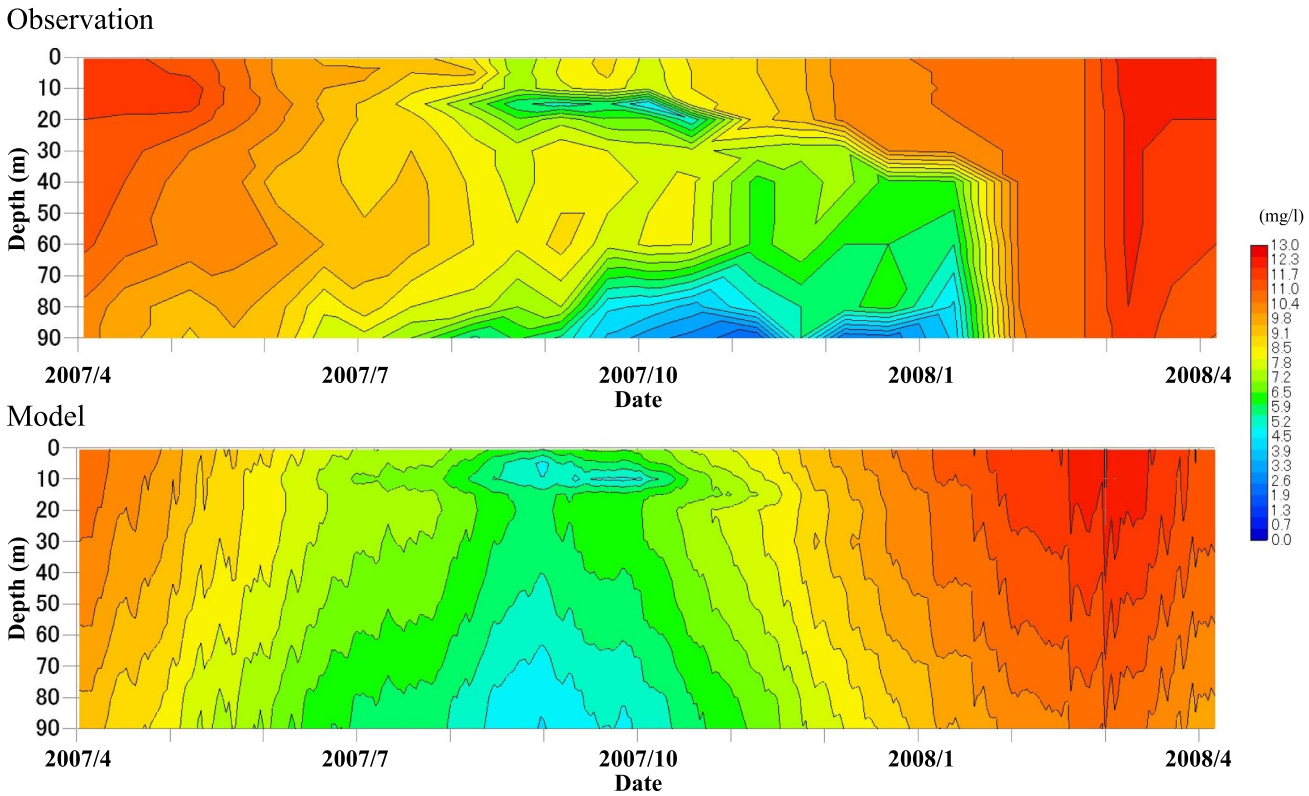

(a) Seasonal change of vertical distribution of Dissolved Oxygen in 2007

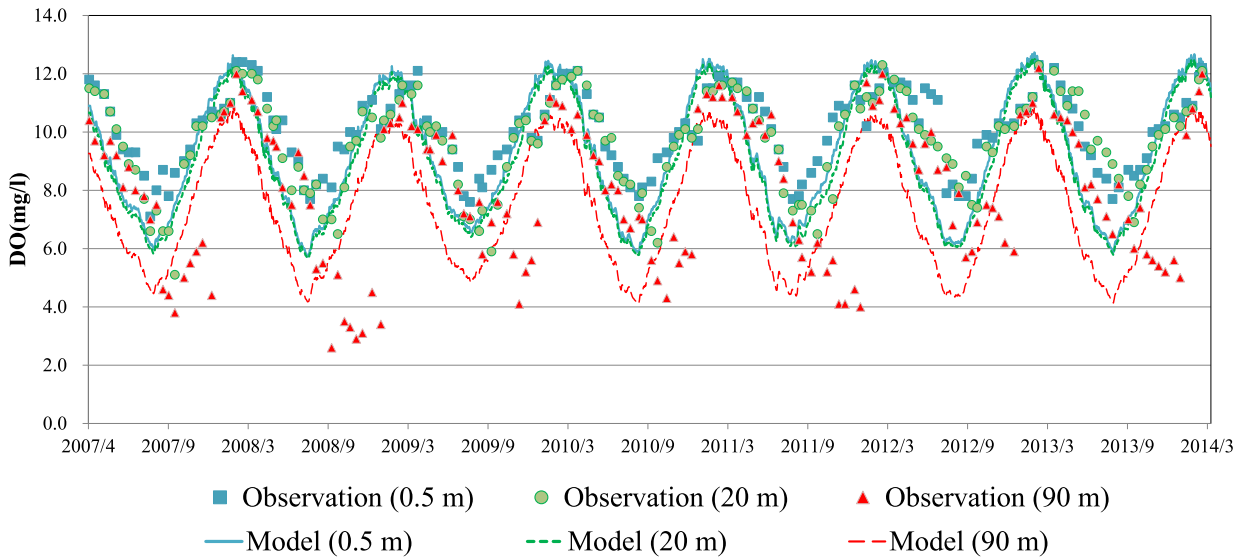

(b) Inter-annual change of vertical distribution of Dissolved Oxygen

Fig. 4 Seasonal and inter-annual change of vertical distribution of observed and simulated DO at Imazu-oki

with oxygen concentrations decreasing year by year compared to the baseline case, and the decrease in dissolved oxygen concentrations to − 0.5 mg/L in winter was due to the increase in water temperature due to mixing with the layer immediately above due to the full layer circulation that occurred in winter, which caused the saturated dissolved oxygen concentration to decrease. The saturated dissolved oxygen concentration decreased due to a fall in the water temperature caused by mixing with the layer directly above, which occurred in winter. When wind

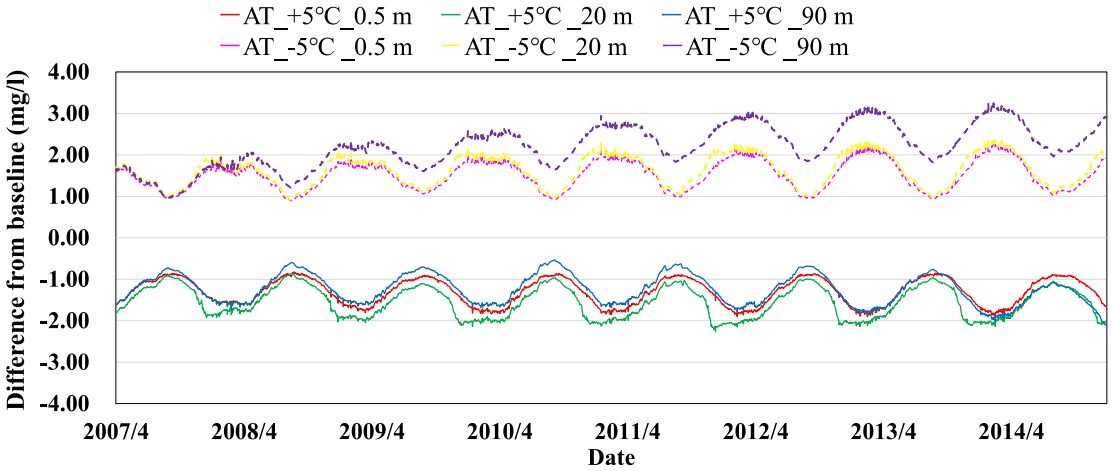

Fig. 5 Inter-annual change of difference of DO between BASE and AT_±5 ℃ in the surface layer (0 m depth), thermocline (20 m depth) and deep layer (90 m depth) from 2007 to 2014 at Imazu-oki

Fig. 6 Inter-annual change of difference of DO between BASE and WS_double, or half in the surface layer (0 m depth), thermocline (20 m depth) and deep layer (90 m depth) from 2007 to 2014 at Imazu-oki

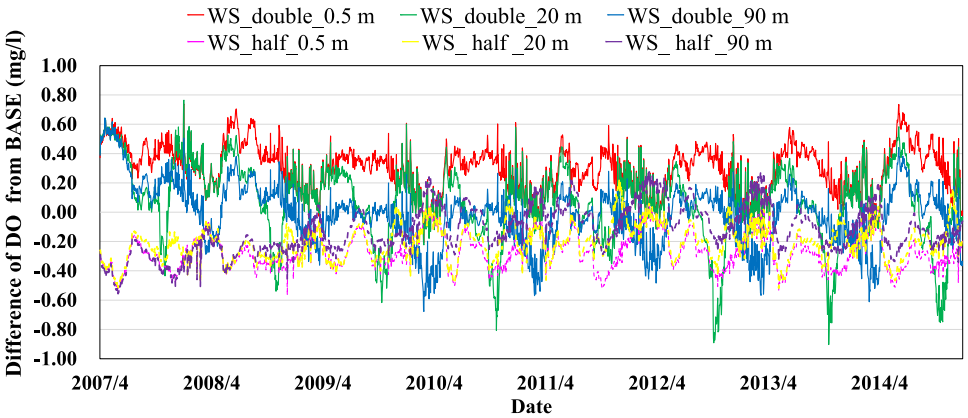

speed was reduced by a factor of 1/2, wind stirring in the surface and thermocline decreased, oxygen supply from the atmosphere decreased and dissolved oxygen concentration decreased by − 0.1 mg/L. Dissolved differential concentrations in the bottom layer remained almost unchanged.

Figure 7 shows the interannual variation of the dissolved oxygen concentration difference between the case with varying precipitation and the baseline case from 2007 to 2014. It was shown that dissolved oxygen concentrations remained almost unchanged from the surface to the bottom layer when precipitation increased by a factor of 2 and decreased by a factor of 1/2. In particular, changes in precipitation are an issue because the one-dimensional model developed this time does not take into account the load caused by river inflows, since nutrient concentrations and lake water temperature also change depending on the amount of inflow from the river.

4 Conclusion

The IPCC Sixth Assessment Report on Climate Change discusses several scenarios using the SSP, of which SSP5-8.5 has the greatest impact on temperatures, with a projected temperature increase of 3.3–5.7 °C. This scenario indicates an increase in the frequency of tropical cyclones over the Southern Ocean, with the potential for significant fluctuations in wind speeds and precipitation.

Based on these conditions, the effects of changes in temperature, wind speed and precipitation on dissolved oxygen concentrations in Lake Biwa were investigated using a one-dimensional model that takes into account the redox reaction of bottom sediment. When air temperature increased by 5 °C, dissolved oxygen concentrations in the surface layer, the thermocline and the bottom layer decreased to different degrees, and conversely tended to increase when air temperature decreased by 5 °C. A

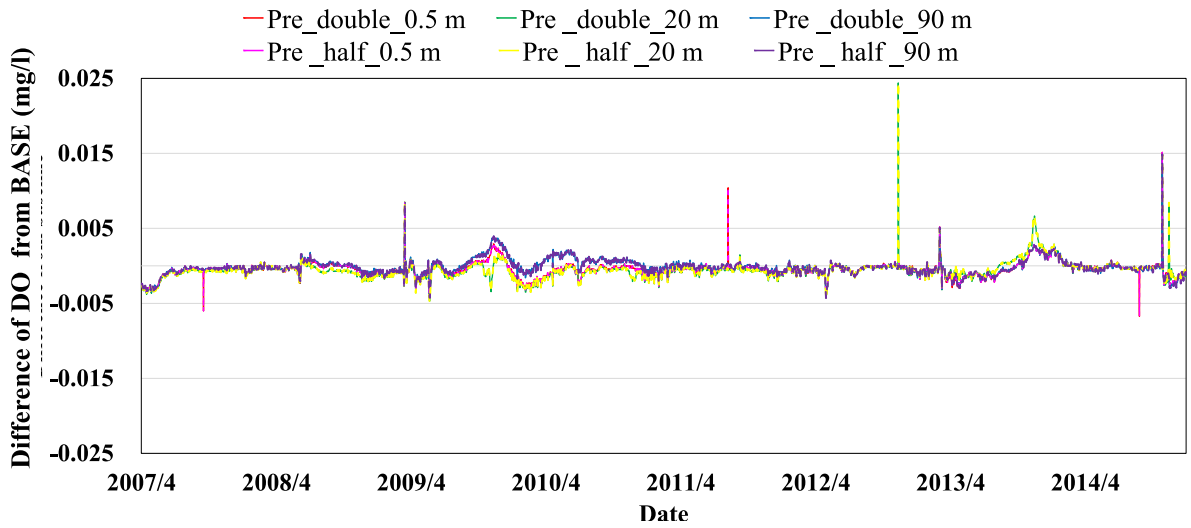

Fig. 7 Inter-annual change of difference of DO between BASE and Pre_double, or half in the surface layer (0 m depth), thermocline (20 m depth) and deep layer (90 m depth) from 2007 to 2014 at Imazu-oki

doubling of wind speed increased dissolved oxygen concentrations in the surface layer and decreased concentrations in the bottom layer. In the bottom layer, mixing with the layer immediately above was considered to increase water temperature, decrease saturated dissolved oxygen concentrations and decrease oxygen concentrations. The effect of wind speed varies with the season, with a significant increase in oxygen concentration in the surface layer from summer to autumn, and from autumn to winter, vertical mixing from the surface to the bottom layer, accelerated by the wind, causes the water mass in the lake bottom to mix with the layer directly above, increasing water temperature, decreasing saturated dissolved oxygen concentration and decreasing oxygen concentration. This phenomenon affects the oxygen cycle throughout the lake.

The lake's response to changes in precipitation was shown to be limited and largely unchanged. This suggests that in future climate change, the effect of precipitation fluctuations on the oxygen concentration in Lake Biwa will be relatively small, and that interactions with other meteorological factors will be important.

In this study, seasonal interannual changes were analyzed for long-term analysis using a one-dimensional model, but in order to accurately predict the future water environmental conditions of Lake Biwa and adapt water quality management, analysis using a three-dimensional model that comprehensively considers not only meteorological factors but also the characteristics of the lake itself and geographical factors is necessary. Particularly with regard to changes in precipitation, as nutrient levels and lake water temperature also vary depending on the inflow from rivers, a comprehensive approach combining these diverse factors is essential for sustainable water resources management.

Funding Open Access funding provided by Kobe University. This research was partially performed by the Environment Research and Technology Development Fund (2RL-2301) of the Environmental Restoration and Conservation Agency provided by Ministry of the Environment of Japan.

Data availability The datasets generated and analyzed during the current study are available from the corresponding author on reasonable request.

Declarations

Conflict of interest The author declared that he has no conflict of interest.

References

Byrne M, Hernández JC (2020) Chapter 16—Sea urchins in a high CO_2 world: Impacts of climate warming and ocean acidification across life history stages. Dev Aquac Fish Sci. 43:281–297. https://doi.org/10.1016/B978-0-12-819570-3.00016-0

Cheng L, Abraham J, Goni G, Boyer T, Wijffels S, Cowley R, Gouretski V, Reseghetti F, Kizu S, Dong S et al (2016) XBT

Science: Assessment of instrumental biases and errors. Bull Am Meteorol Soc. 97(6):924–933. https://doi.org/10.1175/BAMS-D-15-00031.1

Christianson KR, Johnson BM, Hooten MB (2020) Compound effects of water clarity, inflow, wind and climate warming on mountain lake thermal regimes. Aquat Sci. 82:6. https://doi.org/10.1007/s00027-019-0676-6

Desgué-Itier O, Soares LMV, Anneville O, Bouffard D, Chanudet V, Danis PA, Domaizon I, Guillard J, Mazure T, Sharaf N, Soulignac F, Tran-Khac V, Vinçon-Leite B, Jenny JP (2023) Past and future climate change effects on the thermal regime and oxygen solubility of four peri-alpine lakes. Hydrol Earth Syst Sci. 27:837–859. https://doi.org/10.5194/hess-27-837-2023

Detmer TM, Parkos JJ, Wahl DH (2022) Long-term data show effects of atmospheric temperature anomaly and reservoir size on water temperature, thermal structure, and dissolved oxygen. Aquat Sci. 84:3. https://doi.org/10.1007/s00027-021-00835-2

Durack PJ, Gleckler PJ, Purkey SG et al (2018) Ocean warming: from the surface to the deep in observations and models. Oceanography. 31(2):41–51. https://doi.org/10.5670/oceanog.2018.227

Findlay HS, Turley C (2021) Chapter 13—Ocean acidification and climate change, climate change, 3rd edn. Elsevier, Amsterdam.

Fueglistaler S, Silvers LG (2021) The peculiar trajectory of global warming. J Geophys Res Atmos. 126:e2020JD033629.

Henson SA, Cael BB, Allen SR et al (2021) Future phytoplankton diversity in a changing climate. Nat Commun. 12:5372. https://doi.org/10.1038/s41467-021-25699-w

IPCC (2022) Climate change 2022: Impacts, adaptation, and vulnerability. Contribution of working group II to the sixth assessment report of the intergovernmental panel on climate change Cambridge University Press, Cambridge, UK and New York, NY, USA. https://doi.org/10.1017/9781009325844

Jevrejeva S, Jackson LP, Riva REM, Grinsted A, Moore JC (2016) Coastal sea level rise with warming above 2 ℃. Proc Natl Acad Sci USA. 113:342–347. https://doi.org/10.1073/pnas.1605312113

Johnson GC, Lyman JM (2020) Warming trends increasingly dominate global ocean. Nat Clim Chang.10:757–761. https://doi.org/10.1038/s41558-020-0822-0

Koue J, Shimadera H, Matsuo T, Kondo A (2018) Evaluation of thermal stratification and flow field reproduced by a three-dimensional hydrodynamic model in Lake Biwa. Jpn Water. 10(1):47. https://doi.org/10.3390/w10010047

Koue J, Shimadera H, Matsuo T, Kondo A (2020) Numerical simulation for seasonal and inter-annual change of dissolved oxygen in Lake Biwa, Japan. Int J Geomate. 18(66):56–61. https://doi.org/10.21660/2020.66.9366

Perlov D, Reavie ED, Quinlan R (2023) Anthropogenic stressor impacts on hypolimnetic dissolved oxygen in Lake Erie: A chironomid-based paleolimnological assessment. J Great Lakes Res. 49(5):953–968. https://doi.org/10.1016/j.jglr.2023.04.006

Rabalais NN, Turner RE, Díaz RJ, Justić D (2009) Global change and eutrophication of coastal waters. ICES J Mar Sci. 66(7):1528–1537. https://doi.org/10.1093/icesjms/fsp047

Robins PE, Lewis JW, Simpson JH, Howlett ER, Malham SK (2014) Future variability of solute transport in a macrotidal estuary. Estuar Coast Shelf Sci. 151:88–99. https://doi.org/10.1016/j.ecss.2014.09.019

Ross AC, Najjar RG, Li M, Mann ME, Ford SE, Katz B (2015) Sea-level rise and other influences on decadal-scale salinity variability in a coastal plain estuary. Estuar Coast Shelf Sci. 157:79–92. https://doi.org/10.1016/j.ecss.2015.01.022

Scavia D, Field JC, Boesch DF et al (2002) Climate change impacts on U.S. Coast Mar Ecosyst Estuar. 25:149–164. https://doi.org/10.1007/BF02691304

Smucker NJ, Beaulieu JJ, Nietch CT, Young JL (2021) Increasingly severe cyanobacterial blooms and deep water hypoxia coincide with warming water temperatures in reservoirs. Glob Change Biol. 27:2507–2519. https://doi.org/10.1111/gcb.15618

Statham PJ (2012) Nutrients in estuaries—An overview and the potential impacts of climate change. Sci Total Environ. 434:213–227. https://doi.org/10.1016/j.scitotenv.2011.09.088

Stetler JT, Girdner S, Mack J, Winslow LA, Leach TH, Rose KC (2021) Atmospheric stilling and warming air temperatures drive long-term changes in lake stratification in a large oligotrophic lake. Limnol Oceanogr. 66:954–964. https://doi.org/10.1002/lno.11654

Tebaldi C, Ranasinghe R, Vousdoukas M et al (2021) Extreme sea levels at different global warming levels. Nat Clim Chang. 11:746–751. https://doi.org/10.1038/s41558-021-01127-1

Yang Z, Wang T, Voisin N, Copping A (2015) Estuarine response to river flow and sea-level rise under future climate change and human development. Estuar Coast Shelf Sci. 156:19–30. https://doi.org/10.1016/j.ecss.2014.08.015